MOLECULAR AND CELLULAR BIOLOGY, Mar. 2011, p. 1098–1108 Vol. 31, No. 5
0270-7306/11/$12.00 doi:10.1128/MCB.01279-10

TDP-43 Is Directed to Stress Granules by Sorbitol, a Novel Physiological Osmotic and Oxidative Stressor▽

Colleen M. Dewey,[1] Basar Cenik,[1,3] Chantelle F. Sephton,[1] Daniel R. Dries,[1] Paul Mayer III,[1] Shannon K. Good,[1] Brett A. Johnson,[2] Joachim Herz,[1,3,4] and Gang Yu[1]*

Departments of Neuroscience,[1] Molecular Biology,[2] Molecular Genetics,[3] and Neurology and Neurotherapeutics,[4] The University of Texas Southwestern Medical Center at Dallas, Dallas, Texas

Received 6 November 2010/Returned for modification 30 November 2010/Accepted 13 December 2010

TDP-43, or TAR DNA-binding protein 43, is a pathological marker of a spectrum of neurodegenerative disorders, including amyotrophic lateral sclerosis and frontotemporal lobar degeneration with ubiquitin-positive inclusions. TDP-43 is an RNA/DNA-binding protein implicated in transcriptional and posttranscriptional regulation. Recent work also suggests that TDP-43 associates with cytoplasmic stress granules, which are transient structures that form in response to stress. In this study, we establish sorbitol as a novel physiological stressor that directs TDP-43 to stress granules in Hek293T cells and primary cultured glia. We quantify the association of TDP-43 with stress granules over time and show that stress granule association and size are dependent on the glycine-rich region of TDP-43, which harbors the majority of pathogenic mutations. Moreover, we establish that cells harboring wild-type and mutant TDP-43 have distinct stress responses: mutant TDP-43 forms significantly larger stress granules, and is incorporated into stress granules earlier, than wild-type TDP-43; in striking contrast, wild-type TDP-43 forms more stress granules over time, but the granule size remains relatively unchanged. We propose that mutant TDP-43 alters stress granule dynamics, which may contribute to the progression of TDP-43 proteinopathies.

TAR DNA-binding protein 43 (TDP-43) is a highly conserved, ubiquitously expressed RNA-binding protein of the heterogeneous nuclear ribonucleoprotein (hnRNP) family (11, 47, 73). TDP-43 and other hnRNPs are multifunctional proteins that regulate gene expression in both the nucleus and the cytoplasm (47, 75). In the nucleus, TDP-43 binds single-stranded DNA and RNA (10, 11, 19, 20, 49, 62) and can function as both a transcriptional repressor (1, 2, 62) and a splicing modulator (15, 17, 20, 55). Specifically, TDP-43 regulates pre-mRNA splicing by binding mRNA with $(UG)_{6–12}$ sequences (19) and by recruiting other hnRNP proteins into repressive splicing complexes (10, 18, 55). However, as a nucleocytoplasmic shuttling protein (12), TDP-43 also has distinct cytoplasmic functions, including mRNA stabilization (74).

Recent studies indicate that TDP-43 localizes to stress granules (SGs) in response to heat shock, oxidative stress, and chemical inducers of stress (23, 33). SGs are dynamic cytoplasmic structures that are believed to act as sorting stations for mRNAs (5). SG composition and morphology differ according to stress and cell type (5, 39), but some core components are conserved. These core components include the RNA-binding protein TIAR (TIA-1 cytotoxic granule-associated RNA-binding protein-like 1) and the stalled translation initiation complex components eIF3 and eIF4G (44, 45). In contrast, the incorporation of the RNA-binding proteins HuR and hnRNP A1 into SGs differs with the cell type and stress (5, 39). The physiological stressors that cause TDP-43 aggregates and SGs to form—and the cells in which this occurs—remain unresolved. Moreover, very little is known about the function of cytoplasmic TDP-43, a pressing issue, since TDP-43 has been linked to multiple neurodegenerative diseases.

"TDP-43 proteinopathies" encompass a spectrum of neurodegenerative diseases with ubiquitinated aggregates composed primarily of TDP-43 (21, 35). Ubiquitinated TDP-43 is especially prevalent in patients with amyotrophic lateral sclerosis (ALS) and frontotemporal lobar degeneration with ubiquitinated inclusions (FTLD-U). In these diseases, many mutations have been identified within the glycine-rich region (GRR) of TDP-43 (~30 mutations in ALS [37, 48, 51, 63, 66, 69, 72] and 2 in FTLD-U [14, 21, 38, 46]). How TDP-43 contributes to neurodegeneration is not known, but other pathological alterations to TDP-43 implicate aberrant proteolysis, hyperphosphorylation, and misaccumulation in the cytoplasm (7, 16, 21, 35, 59).

It is not clear how genetic mutations in TDP-43 contribute to neurodegeneration at the molecular and cellular levels. Existing evidence is compatible with the hypothesis that TDP-43 proteinopathies arise from a gain of TDP-43 function in the cytoplasm due to its misaccumulation in the cytoplasm. This may indirectly or directly impact its nuclear function, since cytoplasmic misaccumulation would reduce the amount of functional TDP-43 in the nuclear compartment. In this study, as a first step toward testing this hypothesis, we build a robust, quantitative, and physiologically relevant cellular model that allows us to establish the conditions under which TDP-43 accumulates in the cytoplasm, such as those seen in TDP-43 proteinopathies. We show that elevated levels of the sugar sorbitol, an intermediate in the polyol pathway (an ATP-independent metabolic route that generates fructose from glucose) (22), result in TDP-43 localization to SGs in Hek293T cells

* Corresponding author. Mailing address: Department of Neuroscience, University of Texas Southwestern Medical Center, 6000 Harry Hines Blvd., Dallas, TX 75390-9111. Phone: (214) 648-5157. Fax: (214) 648-1801. E-mail: Gang.Yu@UTSouthwestern.edu.

▽ Published ahead of print on 20 December 2010.

and, similarly, in primary cultured glia. Furthermore, we use this new cellular model to examine the dynamic assembly of TDP-43$^+$ SGs, including the control of SG size and the molecular determinants within TDP-43 necessary for its assembly into SGs. Finally, we use this model to distinguish between the responses of wild-type TDP-43 and pathological mutant TDP-43 to stress. Mutant TDP-43 variants are incorporated into stress granules earlier than wild-type TDP-43, and these mutants form significantly larger stress granules. In striking contrast, wild-type TDP-43 forms more cytoplasmic granules over time, but the granule size remains relatively unchanged. Thus, we establish in this study a simple yet rigorous quantitative, physiologically relevant measurement of TDP-43 aggregate formation *in vivo*, and we use our novel assay to identify the regions of TDP-43 that contribute to this pathological phenomenon.

MATERIALS AND METHODS

Constructs and primers. We used TDP-43 mouse cDNA (Image clone 5346061) as a template with primers 5′-(HindIII) (TTTAAGCTTATGTCTGAATATATTCGGGTAACAGAAGATGAGAACG) and 3′-(BamHI) (TTTGGATCCCATTCCCCAGCCAGAAGACTTAGAATCCATGC) (restriction enzyme sites are underlined). The insert was sequentially digested with BamHI and HindIII and was subcloned into the pcDNA4 myc-His B vector (Invitrogen) to generate TDP-43 with C-terminal myc and 6×His tags. Site-directed mutagenesis on the pcDNA4B-TDP-43 template was used to generate the following mutations with the primers given in parentheses by using QuikChange (Qiagen): G348C (5′-CAGCAGAACCAGTCGTGCCCATCTGGGAATA and 3′-TATTCCCAGATGGGCACGACTGGTTCTGCTG), A315T (5′-GGATGAACTTTGGTACTTTTAG CATTAACC and 3′-GGTTAATGCTAAAAGTACCAAAGTTCATCC), G294A (5′-GGTAACAGTAGAGCG GGTGGAGCTGGCTTGG and 3′-CCAAGCCAGCTCCACCCGCTCTACTGTTACC), and N390S (5′-GTTGGGGGTCAGCATCAAGTGCAGGATCGG and 3′-CCGATCCTGCACTTGATGCTGACCCCCAAC). The following truncated TDP-43 constructs were subcloned into the pcDNA4b vector using HindIII and BamHI with the primer sets given in parentheses: construct 1-114 (5′-TTTAAGCTTATGTCTGAATATATTCGGGTAACAGAAGATGAGAACG and 3′-TTTGGATCCTTTCCAGGGGAGACCCAACACTATGAGGTCAGATGTTTTCTGGAC), construct 1-179 (5′-TTTAAGCTTATGTCTGAATATATTCGGGTAACAGAAGATGAGAACG and 3′-TTTGGATCCGTTGGGAAGTTTACAGTCACACCATCGCCCATCTATCATATGTCG), construct 1-267 (5′-TTTAAGCTTATGTCTGAATATATTCGGGTAACAGAAGATGAGAACG and 3′-TTTGGATCCATTGCTATTATGCTTAGGTTCAGCATTGGATATATGCACGCTGAT), and construct 1-324 (5′-TTTAAGCTTATGTCTGAATATATTCGGGTAACAGAAGATGAGAACG and 3′-TTTGGATCCAGCCATCATCGCTGGGTTAATGCTAAAAGCACCAAAGTTCATCCC). Sequences were confirmed by the University of Texas (UT) Southwestern sequencing facility using T7 and BGH primers.

Cells and primary cultures. The Hek293T cell lines used in this study were maintained in standard growth medium: 10% fetal bovine serum in Dulbecco's modified Eagle medium (DMEM) (Invitrogen). Low-passage-number cells were used for analyzing stress granule formation due to their robust response to stress. For primary mixed glial cultures, rat cortices were dissected from postnatal (days 1 to 4 [D1 to D4]) pups in ice-cold dissection medium (Gibco-Invitrogen) as described previously (67). Glia (~21 to 28 days *in vitro* [DIV]) were split onto poly-D-lysine- and Matrigel-coated coverslips and were subjected to stress with 0.4 M sorbitol (Sigma) the next day.

Transfection and stable cell selection. pcDNA4B-TDP-43-myc/6×-His and pcDNA4B-TDP-43-G348C-myc/6×-His were transfected into Hek293T cells with Fugene HD (Roche) according to the manufacturer's instructions. After 2 days, 800 μg ml^{-1} zeocin was added to the growth medium to select for transformants. Following selection, cells were maintained in 400 μg ml^{-1} zeocin growth medium.

Induction of osmotic stress and TDP-43 clustering optimization. D-Sorbitol (Sigma) was diluted in standard growth medium to yield a 0.4 M concentration. For Hek293T cells, optimal endogenous TDP-43 clustering was observed between passages 3 and 8. In stable cell lines, we observed robust TDP-43 clustering 6 to 8 passages after zeocin selection. For all experiments, immunofluorescent validation of cellular TDP-43 clustering was performed alongside Western blot analysis.

shRNA-mediated knockdown of TDP-43. Sigma Mission short hairpin RNAs (shRNAs) against human TDP-43 (NM_007375) were purchased precloned into the backbone vector plko.1 puro. shRNA constructs (constructs 1261, 666, 1333, 931, and 177) were cotransfected with helper plasmids pspax2 and VSVG using Fugene HD (Roche) according to the manufacturer's specifications. Optimal knockdown of TDP-43 was obtained using shRNA plasmid 1333, and stable selection of virus-infected cells was achieved using 1 μg ml^{-1} puromycin (Sigma). Control stable cell lines expressing shRNA directed against enhanced green fluorescent protein (EGFP) (Sigma) were generated.

Poly(ADP-ribose) polymerase (PARP) cleavage and Western blotting. Hek293T cells were seeded into 10-cm-diameter plates at night and were subjected to 0.4 M sorbitol stress the following day alongside an untreated control. Cells were resuspended in a high-salt buffer (50 mM Tris-HCl [pH 7.5], 0.5 M NaCl, 1% NP-40, 1% deoxycholate [DOC], 0.1% sodium dodecyl sulfate [SDS], 2 mM EDTA, and 1 Roche Complete protease inhibitor tablet), freeze-thawed in liquid nitrogen, and sonicated using a Diagenode Bioruptor on the high setting; lysates were precleared by centrifugation at 4°C (14,000 × *g*). Protein was quantified using the Pierce bicinchoninic acid (BCA) reagent; 75 μg of protein was loaded per lane.

Cell viability assay. Hek293T cells were plated at 20,000/well in a 96-well plate. The next day, an MTS [3-(4-5-dimethylthiazol-2-yl)-5-(3-carboxymethoxyphenyl)-2-(4-sulfophenyl)-2H-tetrazolium salt] assay was performed using the CellTiter 96 Aqueous Non-Radioactive Cell Proliferation Assay kit (Promega). Experiments were conducted in triple quadruplicates, according to the manufacturer's protocol. To analyze the recovery of cells after stress, stress was applied for 0.5, 1, 2, or 4 h and the medium was then washed off. The medium was immediately supplemented with the phenozine methosulfate (PMS)-MTS reagent, and a baseline reading was determined after 4 h of color development. This assay was repeated 24 and 48 h into the recovery, and the percentage of cellular viability was determined as 100 × (A_{490} for stressed cells/A_{490} for unstressed cells).

Immunocytochemistry. Briefly, Hek293T cells were plated at 0.50 × 10^5 to 1.0 × 10^5 cells well^{-1} onto nitric acid-etched coverslips coated with poly-D-lysine and Matrigel. Cells were stressed with 0.4 M sorbitol (Sigma) medium for 0.5, 1, 2, or 4 h. Cells were fixed for 15 min with 4% paraformaldehyde (PFA)–2% sucrose–phosphate-buffered saline (PBS) at room temperature and were permeabilized for 5 min with 0.25% Triton X-100 or for 3 min with 100% methanol. Coverslips were blocked for 1 h in 10% normal goat serum in PBS (Jackson ImmunoResearch and Vector Labs). Primary antibodies were used at the following dilutions overnight at 4°C: anti-TDP-43, 1:200 (polyclonal; ProteinTech Group); TDP-43 C-terminal antibody (polyclonal; clone 748C; in-house), 1:500; anti-myc, 1:500 (monoclonal; Santa Cruz) and 1:5,000 (polyclonal; Abcam); anti-hnRNP A1, 1:3,200 (monoclonal; Sigma); anti-HuR, 1:100 (monoclonal; Santa Cruz); and anti-TIAR, 1:500 (BD Transduction Laboratories). The next day, secondary antibodies and dyes were incubated for 30 min at room temperature at the following dilutions: Alexa Fluor 488 goat anti-rabbit, Alexa Fluor 546 goat anti-rabbit, Alexa Fluor 488 goat anti-mouse, and Alexa Fluor 546 goat anti-mouse antibodies, 1:250; rhodamine-conjugated phalloidin, 1:500; and To-Pro-3, 1:1,000 (Invitrogen). All antibodies and dyes were diluted in 3% normal goat serum in PBS. Coverslips were mounted in ProLong Gold antifade reagent (Invitrogen).

Microscopy and image processing. Images were collected on a Zeiss LSM 510 confocal microscope using LSM software. Images were analyzed using ImageJ, MetaMorph, and Zen 2007 Light Edition software. The cytoplasmic granule size was quantified with two programs: Metamorph and ImageJ. Nuclei were quantified using the ImageJ "cell counter" plug-in. Nuclear subtraction was performed in MetaMorph, and images were further processed in ImageJ. The ImageJ plug-in "analyze particles" was used to filter the granule size (size, 0 to 25 pixels^2). The ImageJ plug-in "distribution" then determined the total area of cytoplasmic puncta and the total number of puncta. The average granule size was then calculated as (area of puncta)/(number of puncta). The number of granules per cell was calculated as (number of puncta)/(number of nuclei). The percentage of cells with stress granules was calculated as 100 × [(number of cells with TDP-43$^+$ granules)/(number of nuclei)].

Statistical analysis. All data are the results of at least three independent experiments. All results are recorded/graphed as the means ± standard errors of the means (SEM). *P* values are coded as follows: not significant (NS), >0.05; *, <0.05; **, <0.01; and ***, <0.001. For the endogenous TDP-43 study and transient transfections, Excel and GraphPad Prism were used to log data, determine statistical significance, and graph data. Statistical significance was determined by Student's *t* test (Excel), one-way analysis of variance (ANOVA), two-

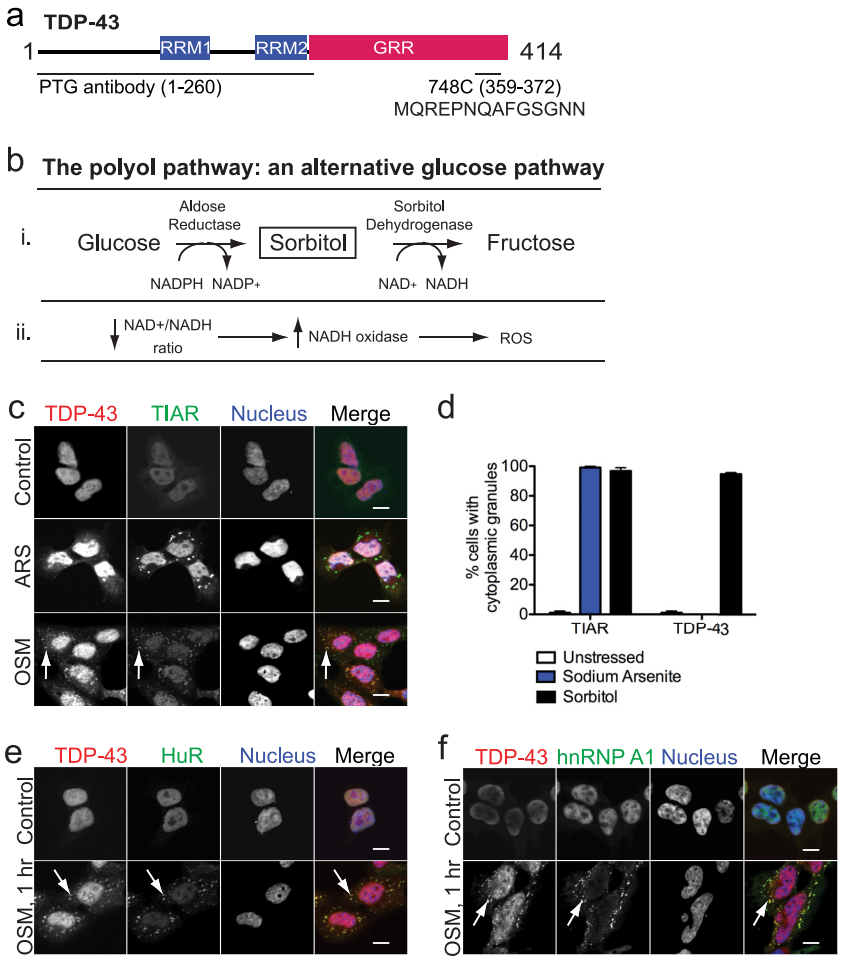

FIG. 1. Hyperosmotic stress is a novel stressor that directs TDP-43 to stress granules. (a) Schematic of TDP-43 structural domains. RRM, RNA recognition motif; GRR, glycine-rich region. Also shown are the epitopes of two antibodies, the ProteinTech Group (PTG) antibody and an in-house C-terminal anti-TDP-43 antibody, 748C. (b) (i) Outline of an alternative glucose-processing pathway, the polyol pathway. (ii) Typically recognized as an osmotic stressor, sorbitol is also an oxidative stressor, through the sorbitol dehydrogenase reaction shown in panel i. ROS, reactive oxygen species. (c) TDP-43 forms cytoplasmic granules (arrows) in Hek293T cells in response to sorbitol (osmotic stressor [OSM]) stress but not to sodium arsenite (ARS) (oxidative stressor) stress. (d) Quantification of TDP-43$^+$ and TIAR$^+$ granules in Hek293T cells stressed for 1 h with sorbitol or sodium arsenite as shown in panel c. Data are the results for three experimental sets and are presented as means ± SEM. (e and f) Osmotic stress of Hek293T cells directs TDP-43 to HuR-containing (e) and hnRNP A1-containing (f) stress granules. Bars, 10 μm.

way ANOVA, and Bonferroni multiple-comparison posttests (Prism) where appropriate. For analysis of stable cell lines expressing wild-type and mutant TDP-43, statistical significance was determined using the R software package, version 2.6.0. The significance of the average granule size was determined using the Wilcoxon rank sum test with continuity correction, using a one-sided *P* value. The statistical significance of the number of puncta per cell was determined using Excel and Student's *t* test.

RESULTS

Sorbitol is a novel physiological stressor that directs TDP-43 to stress granules in Hek293T cells and primary cultured glia. TDP-43 is structurally similar to hnRNP A1: both have two RNA recognition motifs (RRM1 and RRM2) and a glycine-rich region (GRR) (Fig. 1a). hnRNP A1 and TDP-43 are nucleocytoplasmic shuttling proteins that can localize to stress granules (SGs) during heat shock and oxidative stress (12, 23, 39, 68). The osmotic and oxidative stressor sorbitol (Fig. 1b) has also been shown to drive hnRNP A1 to SGs (3). Therefore, we tested whether sorbitol could similarly direct TDP-43 to SGs in Hek293T cells, using sodium arsenite (oxidative stress) as a positive control. We chose a 0.4 M sorbitol concentration for low-passage-number Hek293T cells after testing the effects of a range of concentrations (0.2 to 0.8 M) on cellular viability by using the MTS assay and on the ability to induce TDP-43$^+$ granules by using immunofluorescence (results not shown). TDP-43$^+$ granules formed in response to 0.4 M sorbitol stress in Hek293T cells but not in response to arsenite stress (Fig. 1c and d). These TDP-43$^+$ granules colocalized with the stress granule markers HuR and hnRNP A1 (Fig. 1e and f, respectively). Although TDP-43 localizes to SGs in NSC34 cells following a 1-h treatment with 0.5 mM sodium arsenite (23, 39), in Hek293T cells under the same conditions, we failed to detect TDP-43 at TIAR$^+$ stress granules (Fig. 1c and d). Previous studies have shown that the composition of SGs can be distinct in different cell types (4, 5). Cells generate distinct SGs in response to different stressors, and these SGs can appear morphologically distinct (4, 5). This phenomenon is readily ob-

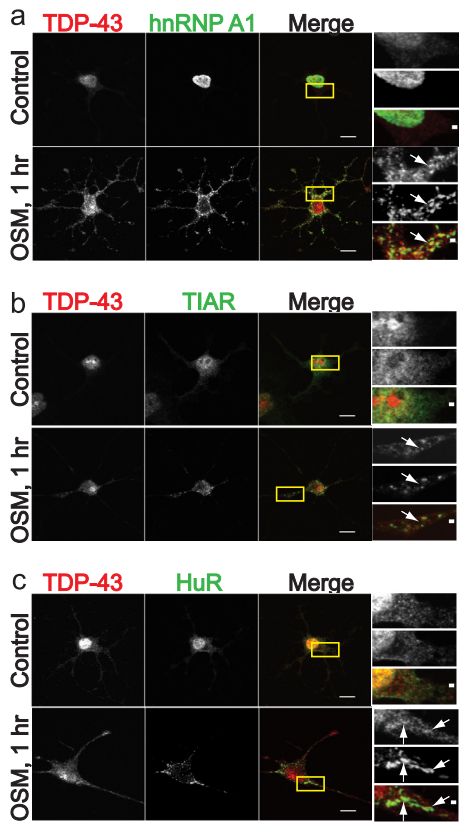

FIG. 2. Hyperosmotic stress directs TDP-43 to stress granules in primary cultured glia. (a to c) Mixed primary cultured glia stressed for 1 h with 0.4 M sorbitol. TDP-43 was detected with the PTG antibody, and nuclei were stained using ToPro-3. Panels on the right show TDP-43 cytoplasmic clustering and colocalization (arrows) with hnRNP A1 (a), TIAR (b), and HuR (c). Bars, 10 mm (left) and 1 μm (right).

served in Fig. 1c, where arsenite and sorbitol stresses generate TIAR$^+$ granules that appear distinct in morphology, as well as in both number and size (unquantified observations from Fig. 1c). Thus, TDP-43 is recruited to SGs during osmotic stress induced by 0.4 M sorbitol but not during oxidative stress induced by 0.5 mM sodium arsenite in Hek293T cells. This indicates that, unlike TIAR, TDP-43 is not a core component of SGs and that its localization to SGs is stressor dependent.

Since the formation of SGs can also be cell type dependent, we next asked whether the sorbitol-induced localization of TDP-43 to SGs also occurs in neural cells. Specifically, we targeted glia, because TDP-43$^+$ pathological inclusions have been observed in glial cells (34). Cortex-derived glia were isolated and subjected to 0.4 M sorbitol stress. TDP-43$^+$ granules were generated after 1 h of stress in multiple types of morphologically distinct glia (Fig. 2a to c). Additionally, these TDP-43$^+$ granules colocalized with the stress granule markers hnRNP A1, TIAR, and HuR (Fig. 2a to c, respectively). Thus, TDP-43 is directed to stress granules by osmotic stress in both Hek293T cells and primary cultured glia. This indicates that in these cells, a common signaling pathway exists that directs TDP-43 to SGs.

The data presented above show that TDP-43 can localize to stress granules in response to specific stress conditions in different cell types. Yet we have no idea of how TDP-43 is incorporated into stress granules over time. How quickly is TDP-43 directed to SGs following an insult? How long does TDP-43 remain associated with stress granules during the stress response? To answer these questions, we exposed Hek293T cells to a time course of 0.4 M sorbitol stress and used immunofluorescence to determine the localization of TDP-43. In unstressed Hek293T cells, TDP-43 is strongly localized to the nucleus (Fig. 3a). Treatment of Hek293T cells with sorbitol, however, showed that by 0.5 h into the stress response, TDP-43 localized to discrete cytoplasmic granules (Fig. 3a, arrows). TDP-43$^+$ granules were observed in some experiments as early as 15 min into the stress response (results not shown). Also, TDP-43 continued to localize to these cytoplasmic granules throughout the stress time course (Fig. 3a, 2 and 4 h). Quantification showed that granule size is relatively uniform from 0.5 to 4 h of sorbitol stress.

As the sorbitol stress continued, we noticed that the cells had a greater number of condensed nuclei (unquantified observations), leading us to speculate that these cells were undergoing apoptosis. Indeed, apoptosis is induced in other cell types following prolonged sorbitol exposure (6, 41, 70). A biological readout of this increased apoptosis is PARP cleavage, which follows caspase-3 activation (61). To determine when Hek293T cells induce apoptosis, we examined PARP cleavage in our stressed lysates. We found PARP cleavage throughout 4 h of stress, with the largest amount of cleavage at 2 and 4 h (Fig. 3d). By 2 and 4 h into the stress response, we also detected a truncated 35-kDa TDP-43 species by using an N-terminal (PTG) anti-TDP-43 antibody. This is significant because TDP-43 is a known caspase-3 target, with an N-terminal cleavage product of 35 kDa (30, 76, 77).

To investigate whether Hek293T cells are irreversibly committed to apoptosis following sorbitol exposure, we performed a cellular recovery assay. We stressed the cells for 0.5 to 4 h and determined cellular viability using an MTS assay. Cells were able to recover from 0.5 and 1 h of sorbitol stress but not from 2 or 4 h of stress (Fig. 3e). Moreover, this recovery from sorbitol-induced stress required TDP-43, as evidenced by the fact that cells did not improve their recovery following stress upon TDP-43 knockdown (Fig. 3f and g). Taken together, our data suggest that sorbitol-induced osmotic and oxidative stress sends TDP-43 to uniformly sized cytoplasmic granules within 30 min of stress and that TDP-43 allows for cellular recovery in response to acute sorbitol stress.

The glycine rich region of TDP-43 is critical for regulating both stress granule association and stress granule size. We next used our novel assay to investigate the structural regions that mediate the association of TDP-43 with cytoplasmic granules. To this end, we generated the following truncated constructs: 1-324 (removal of the distal GRR), 1-267 (removal of the entire GRR), 1-179 (removal of the GRR and RRM2), and 1-114 (removal of the GRR, RRM2, and RRM1) (Fig. 4a and c). Transient transfection of these constructs did not show cytoplasmic granules in unstressed cells (Fig. 4b). Moreover, while wild-type TDP-43 (1-414) clustered modestly following 1 h of stress, construct 1-324 clustered robustly at this time point, whereas shorter constructs failed to do so (Fig. 4b and d). Although wild-type TDP-43 failed to produce robust cytoplasmic clusters in response to 1 h of stress, nuclear clusters

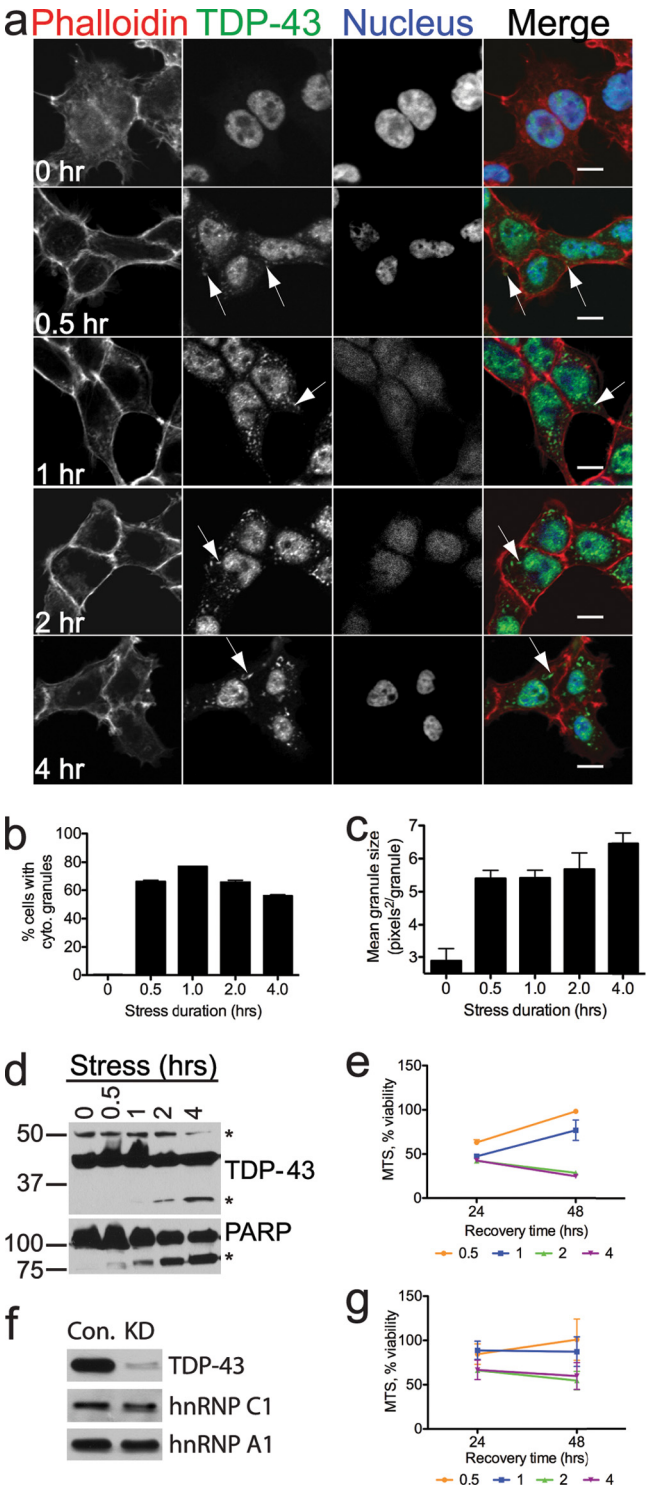

FIG. 3. Characterization of the formation of endogenous TDP-43^{+} stress granules. (a) Immunofluorescence of TDP-43 throughout 4 h of 0.4 M sorbitol administration in Hek293T cells. Arrows highlight TDP-43 cytoplasmic clusters. (b and c) Quantification of cells in panel a. Shown are the percentage of cells with granules (b) and the mean granule size (c). Data are presented as means ± SEM. cyto., cytoplasmic. (d) Prolonged sorbitol stress results in PARP cleavage. (Top) Cross-reactive bands (*) show TDP-43 cleavage products (35 kDa) following 2 to 4 h of stress and a higher-molecular-size TDP-43 species (50 kDa) that declines with longer stress treatment. (Bottom) PARP cleavage (*). (e) Recovery of Hek293T cells from 0.5 to 4 h of sorbitol stress. The percentage of cell viability was determined 24 and 48 h after 0.5, 1, 2, or 4 h of sorbitol stress. Viability was determined using the MTS assay in triplicate, and data are presented as means ± SEM. (f) shRNA-mediated knockdown (KD) of TDP-43 in Hek293T cells. Con., EGFP shRNA control. (g) Recovery of Hek293T cells in which TDP-43 expression was knocked down as in panel f. Experiments were performed in triplicate as for panel e, and data are presented as means ± SEM.

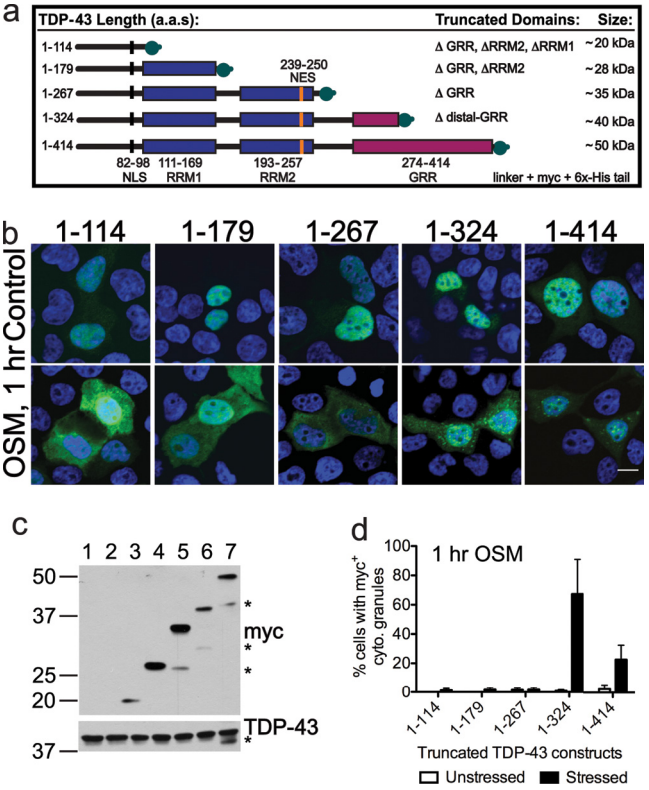

FIG. 4. The cytoplasmic clustering of TDP-43 is mediated by residues 268 to 324. (a) Schematic of truncated TDP-43 constructs with successive deletions in organized structural regions, including the distal C terminus (1-324), the glycine-rich region (GRR) (1-267), RRM2 (1-179), and RRM1 (1-114). NES, nuclear export signal; NLS, nuclear localization signal. (b) Localization of the transiently transfected constructs from panel a following 1 h of sorbitol stress (OSM). Bar, 10 μm. (c) Expression of constructs from panel a in Hek293T cells. Asterisks (*) indicate alternative C-terminal TDP-43 species detected by the anti-myc antibody. Lanes: 1, Venus; 2, pcDNA4b; 3, construct 1-114; 4, construct 1-179; 5, construct 1-267; 6, construct 1-324; 7, construct 1-414. (d) Quantification of cytoplasmic (cyto.) clustering of the truncation constructs following 1 h of stress.

were detected; interestingly, construct 1-324 also showed these nuclear clusters (Fig. 4b). Taken together, these data indicate that the region mediating the association of TDP-43 with stress granules lies within residues 268 to 324.

We should also note, although it is beyond the scope of this investigation, that we noticed additional myc^{+} bands generated from constructs 1-267, 1-32, and 1-414 (Fig. 4c, asterisks). Coincidentally, the sizes of these fragments are in agreement with proposed cleavage site/alternative TDP-43 isoforms

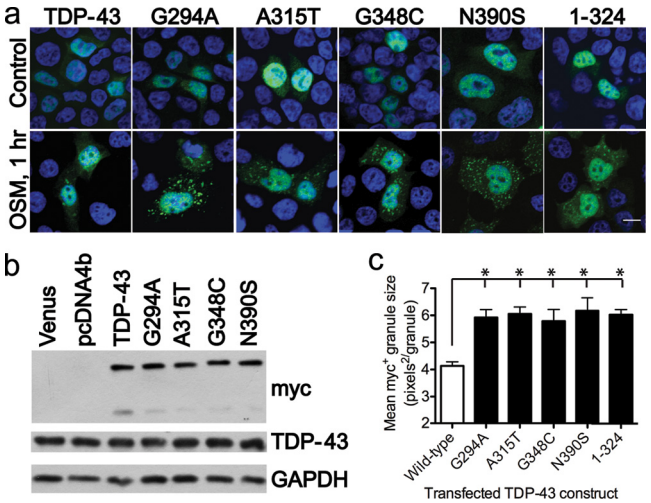

FIG. 5. Alteration of the distal C terminus generates larger cytoplasmic granules than does wild-type TDP-43 in response to stress. (a) Localization of transiently expressed pathological TDP-43 mutants and TDP-43 lacking the distal C terminus in Hek293T cells. Exogenous TDP-43 was stained with the anti-myc antibody; nuclei, with ToPro-3. Bar, 10 μm. (b) Expression of constructs shown in panel a. (c) Quantification of cytoplasmic myc$^+$ granule size (pixels^2/granule) following 1 h of sorbitol stress. Shown are mean granule sizes ± SEM for wild-type (open bar) and mutant (filled bars) TDP-43 (*, $P < 0.05$).

starting at M(85)TED (60, 77) but could also indicate a novel protease that targets TDP-43. The role of these TDP-43 truncations in the sorbitol-induced stress response has been reserved for future study.

Approximately 10 pathological mutations lie within residues 268 to 324, yet nearly 20 pathological mutations lie outside this region. In previous studies, the overexpression of several pathological mutations *in vitro* resulted in no gross localization defects (A315T, G348C, and A382T) (42), no effect on splicing (Q331K, M337V, and G348C) (26), and no effect on protein-protein interactions (A315T and M337V) (33). We hypothesized that wild-type and mutant TDP-43 could be differentiated by their responses to sorbitol stress. To examine the effect of sorbitol stress on pathological TDP-43 mutants, we selected the familial ALS (fALS) mutation A315T (37, 43), the sporadic ALS (sALS) mutation G294A, and the fALS and sALS mutation G348C (27, 29, 43, 48), because they have no overt phenotype in unstressed cells (26, 33, 42). We also overexpressed the sporadic ALS mutation N390S, in addition to wild-type TDP-43, truncated (construct 1-324) TDP-43, and a vector control (Fig. 5b). All these constructs localized predominantly to the nucleus in unstressed Hek293T cells (Fig. 5a), consistent with previous results (42). However, following 1 h of stress, robust cytoplasmic granules were formed by each pathological mutant, while the wild type failed to generate this robust phenotype. Quantification of these myc$^+$ granules revealed that pathological TDP-43 mutants also formed significantly larger cytoplasmic granules than wild-type TDP-43 (Fig. 5c), an observation consistent with the image for truncated TDP-43 construct 1-324 shown in Fig. 4b. Similar effects were also seen at later time points (data not shown). Importantly, nonpathological mutations outside the C terminus (S242A and ^{189}RSR^{191}→AAA) do not produce larger granules (data not shown), confirming the specificity of this observation for pathological mutations in the C terminus. Taken together, our data show that pathological TDP-43 mutants localize more readily to larger cytoplasmic clusters than does wild-type TDP-43.

Mutant TDP-43 localizes to progressively larger stress granules during stress. To further characterize the difference between wild-type and mutant TDP-43-containing SGs, we established stable cell lines overexpressing either wild-type or mutant (G348C) TDP-43, using myc- and C-terminus-specific (748C) antibodies, respectively, to assess the level of overexpression relative to that of endogenous protein (Fig. 6a). We selected the G348C mutation for further study because it is linked with both sALS and fALS, familial mutations found in multiple families with distinct ancestries (27, 29, 43, 48), and because this mutation lies within a specific subregion (residues 321 to 366) of the GRR that mediates interactions with hnRNP A2 (26). Interestingly, we observed a 1.5-fold difference in doubling frequency favoring the growth of stable cell lines overexpressing wild-type TDP-43 over that of cell lines overexpressing the mutant (means ± SEM, 1.54 ± 0.05 for the wild type versus 1.27 ± 0.09 for the G348C mutant; $P < 0.05$ [data not shown]).

We next determined whether mutant TDP-43 localizes to SGs by treating cells with cycloheximide (CHX), a protein synthesis inhibitor that prevents SG assembly. We treated stable cell lines with CHX (40 μg ml^{-1}) or a vehicle control (dimethyl sulfoxide [DMSO]), followed by 1 h of osmotic stress, to examine whether the granule size was affected by the treatments (Fig. 6b and c). After 1 h of stress, exogenous mutant TDP-43 was robustly directed to stress granules, whereas overexpressed wild-type TDP-43 was not. In stable cell lines overexpressing wild-type TDP-43, the stress granule size was consistent with that observed with transient overexpression, roughly 4 pixels^2/granule (Fig. 6c). Cells expressing mutant TDP-43, however, had larger granules that shrank upon treatment with CHX (Fig. 6c, ** [$P < 0.01$]). Additionally, we verified the colocalization of exogenous TDP-43 granules with the stress granule markers hnRNP A1 (Fig. 6d), HuR (Fig. 6e), and TIAR (Fig. 6f). Thus, mutant TDP-43 localizes to larger stress granules than wild-type TDP-43.

Next, stable cell lines overexpressing wild-type and mutant (G348C) TDP-43 were subjected to a time course of stress (0.4 M sorbitol for 0.5, 1, 2, and 4 h). In unstressed cells, both wild-type TDP-43 and mutant TDP-43 were localized primarily to the nucleus (Fig. 7a). In both unstressed stable cell lines and mixed primary glial cultures, we also detected similar background levels of other cytoplasmic granules that resemble the closely related P-bodies (Fig. 7a and data not shown). Determination of the number of cells that generated myc$^+$ granules in response to the stress showed that the localizations of mutant and wild-type TDP-43 were not statistically different before stress (Fig. 7b). However, following 0.5 and 1 h of sorbitol stress, clustering of TDP-43 was found in more mutant-overexpressing than wild-type-overexpressing cells; moreover, this marked difference disappeared at 2 h of treatment (Fig. 7b). Furthermore, while cells expressing wild-type TDP-43 gradually formed more clusters throughout all 4 h of stress, those expressing mutant TDP-43 showed a rapid accumulation of

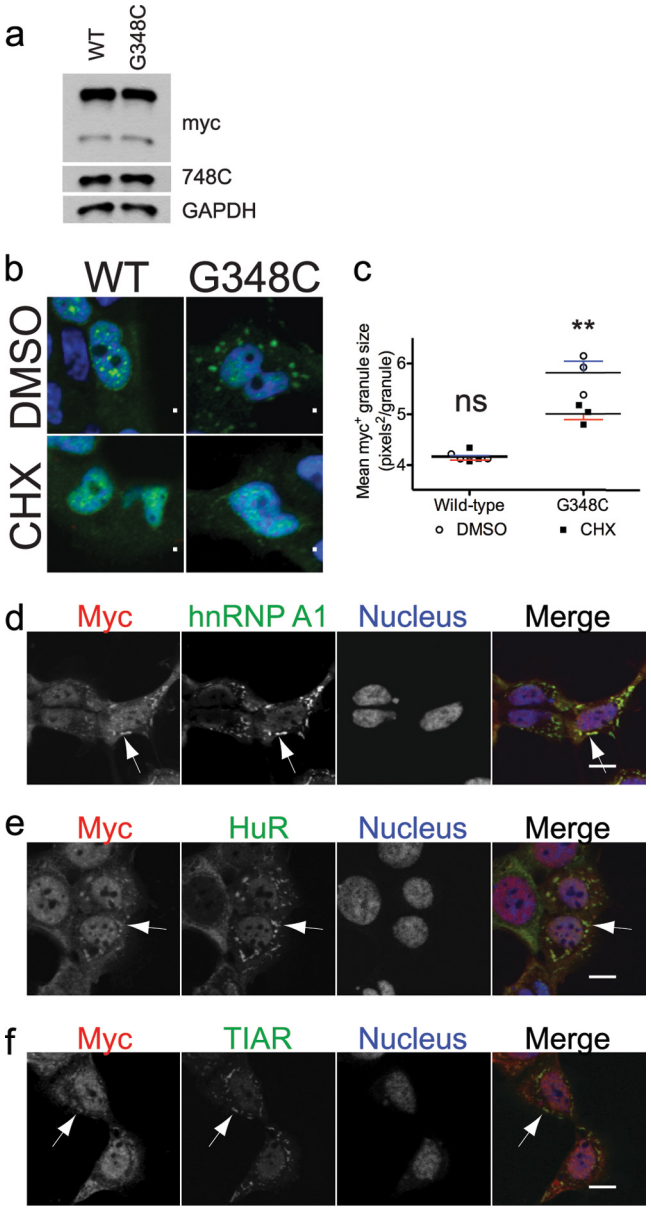

FIG. 6. The pathological TDP-43 G348C mutant localizes to larger stress granules than wild-type (WT) TDP-43 during osmotic stress. (a) Expression levels of myc-tagged WT and mutant (G348C) TDP-43 in stable cell lines. (b) Localization of WT and mutant TDP-43 granules in stressed cells (1 h; sorbitol) treated with CHX or a control (DMSO). (c) Scatter plot of the mean granule sizes in the cells shown in panel b. Horizontal bars indicate the means and SEM (**, $P < 0.01$). Each data point represents the individual mean of a single experiment; the results of three experiments per group are shown. (d to f) Colocalization of mutant (G348C) TDP-43 with hnRNP A1 (d), HuR (e), and TIAR (f) following 1 h of stress. Exogenous mutant TDP-43 was detected using the anti-myc antibody. Bars, 10 μm.

TDP-43 clusters at 0.5 h, followed by a slow decline (Fig. 7c). Importantly, overexpression of mutant TDP-43 resulted in larger sorbitol-induced clusters than overexpression of wild-type TDP-43; this was the most striking difference between sorbitol-induced wild-type and mutant TDP-43 cytoplasmic clusters at all time points (Fig. 7d). Finally, mutant TDP-43 did not induce apoptosis prematurely, as judged by PARP cleavage (Fig. 7e, top); moreover, overexpression of either wild-type or mutant TDP-43 allowed equally for the recovery of cells following as many as 4 h of sorbitol stress (Fig. 7e, bottom).

DISCUSSION

Although quickly expanding, our understanding of transient stress granule structures and their role in disease progression is at a primitive stage. Currently, stress granules are known to contribute to the pathogenesis of several disorders, including fragile-X syndrome, spinal muscular atrophy, and ischemia-reperfusion injury (5, 25, 28); like TDP-43 and FUS/TLS (fused in sarcoma/translated in liposarcoma) proteinopathies, these disorders are caused by altered RNA-binding proteins (4, 5, 24, 25, 28, 54, 75). In this study, we show that sorbitol is a novel stressor mediating TDP-43 and hnRNP A1 localization to TIAR$^+$ and HuR$^+$ stress granules; this was observed in both somatic (Hek293T cells) and nervous system (primary cultured glia) cell types. The finding that colocalization of hnRNP A1 with TDP-43$^+$ granules was conserved between somatic cell lines and primary cultured glia (Fig. 1 and 2) indicates that the readily accessible and common Hek293T cell line can be used to model the stress response initiated in cortex-derived glia. We used this information to develop a cell culture model to quantitatively test the stress response mounted by wild-type TDP-43 and the pathological TDP-43 G294A, A315T, G348C, and N390S mutants, in conjunction with several truncated TDP-43 mutants.

Our analysis indicates that a 57-residue region (residues 268 to 324) spanning the first one-third of the glycine-rich region (GRR) is necessary for the association of TDP-43 with stress granules (Fig. 4). Moreover, removal of the distal 90 residues of GRR (residues 325 to 414) leads TDP-43 to behave like a pathological mutant in terms of its ability to increase stress granule size and facilitate assembly. While the current report was under review, another study using arsenite as a stressor similarly found that pathological TDP-43 mutants enhance their stress-induced localization to stress granules (53). These observations are consistent with the model that the GRR harbors intrinsic determinants of stress granule formation: residues 268 to 324 are necessary for the association of TDP-43 with stress granules, while residues 325 to 414 are necessary, but not sufficient, for regulating this association. In this model, the pathological missense mutations—both inside and outside the distal GRR—negate this regulatory capability, perhaps by changing the structure of TDP-43 in a manner similar to distal truncation of TDP-43. However, we cannot rule out alternative explanations. For example, mutations in TDP-43 may alter the interaction of the GRR with structural components of the stress granules to regulate their size. Yet another explanation would be that these mutations result in the acquisition of an as-yet-unknown gain of function, such as higher toxicity in general, which in turn may result in larger stress granules. Future experiments will address each of these models.

Our work reinforces the notion that the GRR plays a crucial regulatory role in proper TDP-43 function. The GRR has been implicated in the regulation of splicing through hnRNP protein-protein interactions (47) and association with stress granules (23). This domain also harbors the vast majority of known

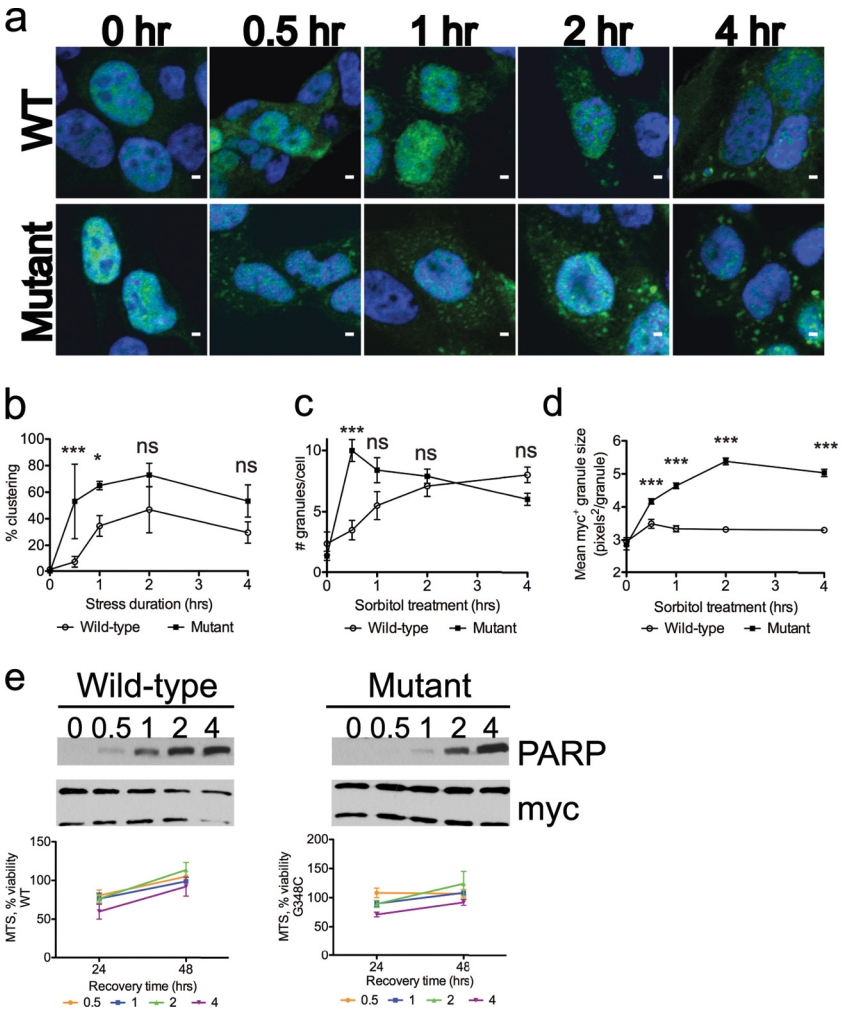

FIG. 7. Wild-type (WT) TDP-43 and a pathological TDP-43 mutant (G348C) form unique stress granules. (a) Localization of exogenous (anti-myc) WT and mutant (G348C) TDP-43 in stably transfected Hek293T cells at the indicated times following sorbitol stress. Bars, 2.5 μm. (b to d) Percentages of stably transfected cells that contain granules (b) and numbers (c) and sizes (d) of granules such as those shown in panel a. Each experiment was performed in triplicate; data are presented as means ± SEM (*, $P < 0.05$; ***, $P < 0.001$). (e) (Top) PARP cleavage throughout 4 h of sorbitol stress. (Bottom) Recovery of stably transfected Hek293T cells expressing wild-type or mutant (G348C) TDP-43. Recovery was measured as for Fig. 3e.

pathological mutations in TDP-43 (and similarly in the pathologically related protein FUS/TLS) (51). The osmotic-stress-responsive sequence (residues 268 to 324 [Fig. 4]) identified in our study overlaps with the oxidative-stress-responsive sequence (residues 216 to 315) previously identified by Colombrita et al. (23). We note, however, that the osmotic-stress-responsive sequence identified here is only half the size of the oxidative-stress-responsive sequence. It is conceivable that the overlapping GRR (residues 268 to 315) of these two stress-responsive sequences in TDP-43 represents a conserved stress response sequence that mediates its association with stress granules in different cell types (both somatic and nervous system specific) and with different stressors (oxidative and osmotic stressors). This region (residues 268 to 315) is particularly glycine rich (Fig. 8a), with multiple putative GXXXG motifs; these motifs are believed to mediate hydrophobic helical protein-protein interactions and have also been found in other proteins involved in neurodegenerative disorders (13, 40). We should also note that while sorbitol can be an oxidative stressor (Fig. 1b), the high concentrations of sorbitol used in this study are typically associated with hyperosmotic stress. Future studies will define the stress-responsive sequence motif in the GRR domain of TDP-43, which may include these GXXXG motifs, and will test whether such a motif is conserved in other GRR-containing proteins, in different cells, and with different stressors.

Since all missense mutations tested in our study mount similar stress responses, we analyzed one of these mutations (G348C) in more detail under progressively longer stress treatments. We found, in comparing cells expressing G348C mutant versus wild-type TDP-43, that a higher percentage of G348C mutant-expressing cells directed the protein into stress granules, that the number of granules formed peaked after a short stress exposure, and that the stress granule size progressively increased at the expense of the number of granules. Yet wild-type TDP-43-expressing cells coped with stress in the converse

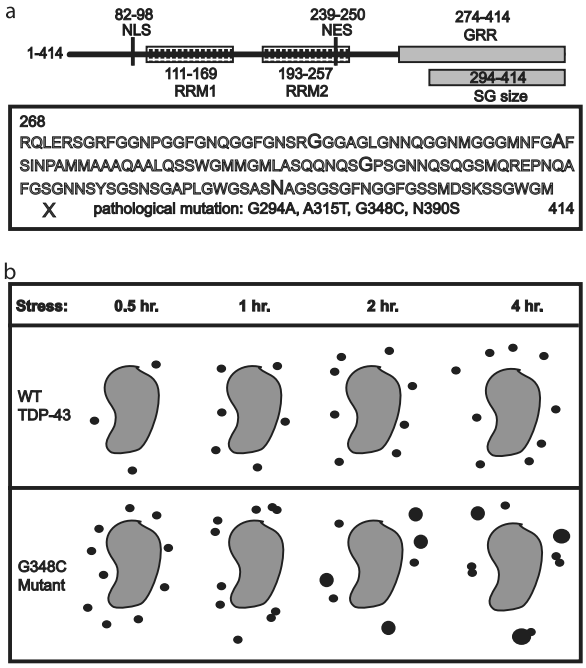

FIG. 8. Model summarizing distinct stress granule species formed by wild-type and mutant (G348C) TDP-43. (a) The GRR harbors putative structural determinants for the association of TDP-43 with stress granules (box) and for the control of stress granule size. NES, nuclear export signal; NLS, nuclear localization signal. (b) Summary of the distinct stress-induced clusters of wild-type and mutant (G348C) TDP-43.

manner: instead of progressively forming larger granules over time, the wild-type protein progressively formed a greater number of smaller granules of relatively unchanged size (Fig. 8b). Our results indicate that the pathological mutant handles stress in a manner markedly different from that of the wild type; these differences will be explored in future studies in order to understand how pathological TDP-43 mutants contribute to neurodegeneration and cell death.

It has been suggested that the formation of stress granules delays apoptosis by sequestering proapoptotic factors (such as RACK1 and ROCK1) (8, 31, 71). Our observation that cells recover after an initial stress response is compatible with this model. However, it is also expected that prolonged stress (beyond the cell's capability to handle such stress) would trigger cell death. Indeed, TDP-43, like PARP, is a target of caspase-3; multiple sites in TDP-43 are reportedly targeted by caspase-3 ($DEND_{10–13}$, $DETD_{85–88}$, and $DVMD_{216–219}$), producing 25- and 35-kDa species (30, 64, 65, 76). In our study, we observed that prolonged sorbitol treatment reduces cell viability, which coincides with the formation of TDP-43$^+$ stress granules in native Hek293T cells (Fig. 3). In spite of the drastically increased stress granule size in cells overexpressing pathological mutants (compared to that for the wild-type protein), we did not observe premature induction of apoptosis in these cells (as indicated by PARP cleavage [data not shown]). We interpret this observation as demonstrating that stress granule size is not a primary determinant of the initiation of apoptosis and that mutants may actually delay the onset of cell death before the host cells commit suicide.

In interpreting our data, we consider that the effect and time course of stress granule formation in cells overexpressing a pathological mutant should best be compared to those in cells overexpressing a wild-type protein. This is particularly relevant when one considers that overexpression of wild-type TDP-43 protein (or several other proteins implicated in neurodegenerative disorders) *in vivo* also promotes TDP-43 pathology and neuronal death over time. In this context, while the general effects are similar, there are subtle differences between the stress response of overexpressed wild-type protein and that of endogenous TDP-43. Another related consideration is that TDP-43 protein levels are likely to be stringently regulated, such that overexpression of TDP-43 alone could cause cell death in some cell types (9). However, at our level of overexpression, we did not observe cell death in unstressed stable cell lines expressing wild-type and mutant TDP-43 (Fig. 7e).

Both neurons and glia display TDP-43$^+$ cytoplasmic aggregates in a spectrum of ALS and FTLD-U neurodegenerative disorders, as well as in a subset of Alzheimer's and Parkinson's diseases (21, 32, 36, 50–52, 58). Degeneration and the eventual death of neurons in these diseases likely reflect a combined outcome of impaired neurons and their supporting glial cells. It is plausible that the neuronal and glial cytoplasmic aggregates in ALS or FTLD-U are end products of stress granules or derivatives of these structures generated after an unsuccessful response to stress. TDP-43 has previously been shown to localize to T-cell-restricted intracellular antigen-1 (TIA-1)-positive stress granules in axotomized C57BL/6 mouse motor neurons (56). While previous studies failed to detect colocalization of TDP-43 with known stress granule markers in patient brain (57) and spinal cord (23) samples, improved techniques now allow the detection of TDP-43 in stress granules in brain samples from ALS and FTLD-U patients (53). Further investigation is needed to analyze the relationship of stress granule formation and TDP-43 proteinopathies in cellular and animal models and in human patients in order to understand the molecular and cellular mechanisms by which TDP-43 and RNA-binding proteins respond to stress in health and disease.

ACKNOWLEDGMENTS

This work was supported by the National Institutes of Health, the Welch Foundation, the Ted Nash Long Life Foundation, the Consortium for Frontotemporal Dementia Research, the American Health Assistance Foundation, and the Humboldt Foundation.

For expert technical assistance, we thank Xinran Liu and Can Cenik. We thank Thomas Südhof for reagents used in this study. Additionally, we thank P. Robin Hiesinger and Kimberly Huber for review of the manuscript. We are also indebted to Matt Higgins and the Farese lab at the Gladstone Institutes for generously and graciously sharing TDP-43 antibodies with us.

REFERENCES

1. **Abhyankar, M. M., C. Urekar, and P. P. Reddi.** 2007. A novel CpG-free vertebrate insulator silences the testis-specific SP-10 gene in somatic tissues: role for TDP-43 in insulator function. J. Biol. Chem. **282:**36143–36154.
2. **Acharya, K. K., C. K. Govind, A. N. Shore, M. H. Stoler, and P. P. Reddi.** 2006. *cis*-requirement for the maintenance of round spermatid-specific transcription. Dev. Biol. **295:**781–790.
3. **Allemand, E., et al.** 2005. Regulation of heterogenous nuclear ribonucleoprotein A1 transport by phosphorylation in cells stressed by osmotic shock. Proc. Natl. Acad. Sci. U. S. A. **102:**3605–3610.
4. **Anderson, P., and N. Kedersha.** 2009. Stress granules. Curr. Biol. **19:**R397–R398.

5. **Anderson, P., and N. Kedersha.** 2008. Stress granules: the Tao of RNA triage. Trends Biochem. Sci. **33:**141–150.
6. **Aquilano, K., et al.** 2007. Reactive oxygen and nitrogen species are involved in sorbitol-induced apoptosis of human erithroleukaemia cells K562. Free Radic. Res. **41:**452–460.
7. **Arai, T., et al.** 2006. TDP-43 is a component of ubiquitin-positive tau-negative inclusions in frontotemporal lobar degeneration and amyotrophic lateral sclerosis. Biochem. Biophys. Res. Commun. **351:**602–611.
8. **Arimoto, K., H. Fukuda, S. Imajoh-Ohmi, H. Saito, and M. Takekawa.** 2008. Formation of stress granules inhibits apoptosis by suppressing stress-responsive MAPK pathways. Nat. Cell Biol. **10:**1324–1332.
9. **Ayala, Y. M., T. Misteli, and F. E. Baralle.** 2008. TDP-43 regulates retinoblastoma protein phosphorylation through the repression of cyclin-dependent kinase 6 expression. Proc. Natl. Acad. Sci. U. S. A. **105:**3785–3789.
10. **Ayala, Y. M., F. Pagani, and F. E. Baralle.** 2006. TDP43 depletion rescues aberrant CFTR exon 9 skipping. FEBS Lett. **580:**1339–1344.
11. **Ayala, Y. M., et al.** 2005. Human, *Drosophila*, and *C. elegans* TDP43: nucleic acid binding properties and splicing regulatory function. J. Mol. Biol. **348:** 575–588.
12. **Ayala, Y. M., et al.** 2008. Structural determinants of the cellular localization and shuttling of TDP-43. J. Cell Sci. **121:**3778–3785.
13. **Barnham, K. J., R. Cappai, K. Beyreuther, C. L. Masters, and A. F. Hill.** 2006. Delineating common molecular mechanisms in Alzheimer's and prion diseases. Trends Biochem. Sci. **31:**465–472.
14. **Borroni, B., et al.** 2009. Mutation within TARDBP leads to frontotemporal dementia without motor neuron disease. Hum. Mutat. **30:**E974–E983.
15. **Bose, J. K., I. F. Wang, L. Hung, W. Y. Tarn, and C. K. Shen.** 2008. TDP-43 overexpression enhances exon 7 inclusion during the survival of motor neuron pre-mRNA splicing. J. Biol. Chem. **283:**28852–28859.
16. **Buratti, E., and F. E. Baralle.** 2009. The molecular links between TDP-43 dysfunction and neurodegeneration. Adv. Genet. **66:**1–34.
17. **Buratti, E., and F. E. Baralle.** 2010. The multiple roles of TDP-43 in pre-mRNA processing and gene expression regulation. RNA Biol. **7:**420–429.
18. **Buratti, E., et al.** 2005. TDP-43 binds heterogeneous nuclear ribonucleoprotein A/B through its C-terminal tail: an important region for the inhibition of cystic fibrosis transmembrane conductance regulator exon 9 splicing. J. Biol. Chem. **280:**37572–37584.
19. **Buratti, E., A. Brindisi, F. Pagani, and F. E. Baralle.** 2004. Nuclear factor TDP-43 binds to the polymorphic TG repeats in CFTR intron 8 and causes skipping of exon 9: a functional link with disease penetrance. Am. J. Hum. Genet. **74:**1322–1325.
20. **Buratti, E., et al.** 2001. Nuclear factor TDP-43 and SR proteins promote in vitro and in vivo CFTR exon 9 skipping. EMBO J. **20:**1774–1784.
21. **Chen-Plotkin, A. S., V. M. Lee, and J. Q. Trojanowski.** 2010. TAR DNA-binding protein 43 in neurodegenerative disease. Nat. Rev. Neurol. **6:**211–220.
22. **Chung, S. S., E. C. Ho, K. S. Lam, and S. K. Chung.** 2003. Contribution of polyol pathway to diabetes-induced oxidative stress. J. Am. Soc. Nephrol. **14:**S233–S236.
23. **Colombrita, C., et al.** 2009. TDP-43 is recruited to stress granules in conditions of oxidative insult. J. Neurochem. **111:**1051–1061.
24. **Cooper, T. A., L. Wan, and G. Dreyfuss.** 2009. RNA and disease. Cell **136:**777–793.
25. **Dahm, R., and P. Macchi.** 2007. Human pathologies associated with defective RNA transport and localization in the nervous system. Biol. Cell **99:** 649–661.
26. **D'Ambrogio, A., et al.** 2009. Functional mapping of the interaction between TDP-43 and hnRNP A2 in vivo. Nucleic Acids Res. **37:**4116–4126.
27. **Daoud, H., et al.** 2009. Contribution of TARDBP mutations to sporadic amyotrophic lateral sclerosis. J. Med. Genet. **46:**112–114.
28. **DeGracia, D. J., J. Rudolph, G. G. Roberts, J. A. Rafols, and J. Wang.** 2007. Convergence of stress granules and protein aggregates in hippocampal cornu ammonis 1 at later reperfusion following global brain ischemia. Neuroscience **146:**562–572.
29. **Del Bo, R., et al.** 2009. TARDBP (TDP-43) sequence analysis in patients with familial and sporadic ALS: identification of two novel mutations. Eur. J. Neurol. **16:**727–732.
30. **Dormann, D., et al.** 2009. Proteolytic processing of TAR DNA binding protein-43 by caspases produces C-terminal fragments with disease defining properties independent of progranulin. J. Neurochem. **110:**1082–1094.
31. **Eisinger-Mathason, T. S., et al.** 2008. Codependent functions of RSK2 and the apoptosis-promoting factor TIA-1 in stress granule assembly and cell survival. Mol. Cell **31:**722–736.
32. **Forman, M. S., J. Q. Trojanowski, and V. M. Lee.** 2007. TDP-43: a novel neurodegenerative proteinopathy. Curr. Opin. Neurobiol. **17:**548–555.
33. **Freibaum, B. D., R. K. Chitta, A. A. High, and J. P. Taylor.** 2010. Global analysis of TDP-43 interacting proteins reveals strong association with RNA splicing and translation machinery. J. Proteome Res. **9:**1104–1120.
34. **Geser, F., et al.** 2008. Evidence of multisystem disorder in whole-brain map of pathological TDP-43 in amyotrophic lateral sclerosis. Arch. Neurol. **65:** 636–641.
35. **Geser, F., V. M. Lee, and J. Q. Trojanowski.** 2010. Amyotrophic lateral sclerosis and frontotemporal lobar degeneration: a spectrum of TDP-43 proteinopathies. Neuropathology **30:**103–112.
36. **Geser, F., et al.** 2009. Clinical and pathological continuum of multisystem TDP-43 proteinopathies. Arch. Neurol. **66:**180–189.
37. **Gitcho, M. A., et al.** 2008. TDP-43 A315T mutation in familial motor neuron disease. Ann. Neurol. **63:**535–538.
38. **Gitcho, M. A., et al.** 2009. TARDBP 3′-UTR variant in autopsy-confirmed frontotemporal lobar degeneration with TDP-43 proteinopathy. Acta Neuropathol. **118:**633–645.
39. **Guil, S., J. C. Long, and J. F. Caceres.** 2006. hnRNP A1 relocalization to the stress granules reflects a role in the stress response. Mol. Cell. Biol. **26:**5744–5758.
40. **Harrison, C. F., et al.** 2010. Conservation of a glycine-rich region in the prion protein is required for uptake of prion infectivity. J. Biol. Chem. **285:**20213–20223.
41. **Izawa, M., and K. Teramachi.** 2001. Down-regulation of protein kinase C activity by sorbitol rapidly induces apoptosis in human gastric cancer cell lines. Apoptosis **6:**353–358.
42. **Kabashi, E., et al.** 2010. Gain and loss of function of ALS-related mutations of TARDBP (TDP-43) cause motor deficits in vivo. Hum. Mol. Genet. **19:**671–683.
43. **Kabashi, E., et al.** 2008. TARDBP mutations in individuals with sporadic and familial amyotrophic lateral sclerosis. Nat. Genet. **40:**572–574.
44. **Kedersha, N., and P. Anderson.** 2007. Mammalian stress granules and processing bodies. Methods Enzymol. **431:**61–81.
45. **Kedersha, N., et al.** 2005. Stress granules and processing bodies are dynamically linked sites of mRNP remodeling. J. Cell Biol. **169:**871–884.
46. **Kovacs, G. G., et al.** 2009. TARDBP variation associated with frontotemporal dementia, supranuclear gaze palsy, and chorea. Mov. Disord. **24:**1843–1847.
47. **Krecic, A. M., and M. S. Swanson.** 1999. hnRNP complexes: composition, structure, and function. Curr. Opin. Cell Biol. **11:**363–371.
48. **Kühnlein, P., et al.** 2008. Two German kindreds with familial amyotrophic lateral sclerosis due to TARDBP mutations. Arch. Neurol. **65:**1185–1189.
49. **Kuo, P. H., L. G. Doudeva, Y. T. Wang, C. K. Shen, and H. S. Yuan.** 2009. Structural insights into TDP-43 in nucleic-acid binding and domain interactions. Nucleic Acids Res. **37:**1799–1808.
50. **Kwong, L. K., K. Uryu, J. Q. Trojanowski, and V. M. Lee.** 2008. TDP-43 proteinopathies: neurodegenerative protein misfolding diseases without amyloidosis. Neurosignals **16:**41–51.
51. **Lagier-Tourenne, C., and D. W. Cleveland.** 2009. Rethinking ALS: the FUS about TDP-43. Cell **136:**1001–1004.
52. **Lagier-Tourenne, C., M. Polymenidou, and D. W. Cleveland.** 2010. TDP-43 and FUS/TLS: emerging roles in RNA processing and neurodegeneration. Hum. Mol. Genet. **19:**R46–R64.
53. **Liu-Yesucevitz, L., et al.** 2010. Tar DNA binding protein-43 (TDP-43) associates with stress granules: analysis of cultured cells and pathological brain tissue. PLoS One **5:**e13250.
54. **Lukong, K. E., K. W. Chang, E. W. Khandjian, and S. Richard.** 2008. RNA-binding proteins in human genetic disease. Trends Genet. **24:**416–425.
55. **Mercado, P. A., Y. M. Ayala, M. Romano, E. Buratti, and F. E. Baralle.** 2005. Depletion of TDP 43 overrides the need for exonic and intronic splicing enhancers in the human apoA-II gene. Nucleic Acids Res. **33:** 6000–6010.
56. **Moisse, K., et al.** 2009. Divergent patterns of cytosolic TDP-43 and neuronal progranulin expression following axotomy: implications for TDP-43 in the physiological response to neuronal injury. Brain Res. **1249:**202–211.
57. **Neumann, M., et al.** 2007. Absence of heterogeneous nuclear ribonucleoproteins and survival motor neuron protein in TDP-43 positive inclusions in frontotemporal lobar degeneration. Acta Neuropathol. **113:**543–548.
58. **Neumann, M., et al.** 2007. TDP-43-positive white matter pathology in frontotemporal lobar degeneration with ubiquitin-positive inclusions. J. Neuropathol. Exp. Neurol. **66:**177–183.
59. **Neumann, M., et al.** 2006. Ubiquitinated TDP-43 in frontotemporal lobar degeneration and amyotrophic lateral sclerosis. Science **314:**130–133.
60. **Nishimoto, Y., et al.** 2010. Characterization of alternative isoforms and inclusion body of the TAR DNA-binding protein-43. J. Biol. Chem. **285:** 608–619.
61. **Obrosova, I. G.** 2005. Increased sorbitol pathway activity generates oxidative stress in tissue sites for diabetic complications. Antioxid. Redox Signal. **7:**1543–1552.
62. **Ou, S. H., F. Wu, D. Harrich, L. F. Garcia-Martinez, and R. B. Gaynor.** 1995. Cloning and characterization of a novel cellular protein, TDP-43, that binds to human immunodeficiency virus type 1 TAR DNA sequence motifs. J. Virol. **69:**3584–3596.
63. **Pesiridis, G. S., V. M. Lee, and J. Q. Trojanowski.** 2009. Mutations in TDP-43 link glycine-rich domain functions to amyotrophic lateral sclerosis. Hum. Mol. Genet. **18:**R156–R162.
64. **Rohn, T. T.** 2008. Caspase-cleaved TAR DNA-binding protein-43 is a major pathological finding in Alzheimer's disease. Brain Res. **1228:**189–198.
65. **Rohn, T. T., and P. Kokoulina.** 2009. Caspase-cleaved TAR DNA-binding

protein-43 in Pick's disease. Int. J. Physiol. Pathophysiol. Pharmacol. **1:**25–32.
66. **Rutherford, N. J., et al.** 2008. Novel mutations in TARDBP (TDP-43) in patients with familial amyotrophic lateral sclerosis. PLoS Genet. **4:**e1000193.
67. **Sephton, C. F., et al.** 2010. TDP-43 is a developmentally-regulated protein essential for early embryonic development. J. Biol. Chem. **285:**6826–6834.
68. **Siomi, H., and G. Dreyfuss.** 1995. A nuclear localization domain in the hnRNP A1 protein. J. Cell Biol. **129:**551–560.
69. **Sreedharan, J., et al.** 2008. TDP-43 mutations in familial and sporadic amyotrophic lateral sclerosis. Science **319:**1668–1672.
70. **Teramachi, K., and M. Izawa.** 2000. Rapid induction of apoptosis in human gastric cancer cell lines by sorbitol. Apoptosis **5:**181–187.
71. **Tsai, N. P., and L. N. Wei.** 2010. RhoA/ROCK1 signaling regulates stress granule formation and apoptosis. Cell. Signal. **22:**668–675.
72. **Van Deerlin, V. M., et al.** 2008. TARDBP mutations in amyotrophic lateral sclerosis with TDP-43 neuropathology: a genetic and histopathological analysis. Lancet Neurol. **7:**409–416.
73. **Wang, H. Y., I. F. Wang, J. Bose, and C. K. Shen.** 2004. Structural diversity and functional implications of the eukaryotic TDP gene family. Genomics **83:**130–139.
74. **Wang, I. F., L. S. Wu, H. Y. Chang, and C. K. Shen.** 2008. TDP-43, the signature protein of FTLD-U, is a neuronal activity-responsive factor. J. Neurochem. **105:**797–806.
75. **Wilkinson, M. F., and A. B. Shyu.** 2001. Multifunctional regulatory proteins that control gene expression in both the nucleus and the cytoplasm. Bioessays **23:**775–787.
76. **Zhang, Y. J., et al.** 2009. Aberrant cleavage of TDP-43 enhances aggregation and cellular toxicity. Proc. Natl. Acad. Sci. U. S. A. **106:**7607–7612.
77. **Zhang, Y. J., et al.** 2007. Progranulin mediates caspase-dependent cleavage of TAR DNA binding protein-43. J. Neurosci. **27:**10530–10534.